Microchim Acta (2014) 181:1999–2008
DOI 10.1007/s00604-014-1293-7

ORIGINAL PAPER

Simultaneous determination of ascorbic acid, dopamine, and uric acid using a carbon paste electrode modified with multiwalled carbon nanotubes, ionic liquid, and palladium nanoparticles

Amir Abbas Rafati · Ahmadreza Afraz · Ali Hajian · Parnaz Assari

Received: 4 March 2014 / Accepted: 13 May 2014 / Published online: 4 June 2014

Abstract We describe the modification of a carbon paste electrode (CPE) with multiwalled carbon nanotubes (MWCNT) and an ionic liquid (IL). Electrochemical studies revealed an optimized composition of 60 % graphite, 20 % paraffin, 10 % MWCNT and 10 % IL. In a next step, the optimized CPE was modified with palladium nanoparticles (Pd-NPs) by applying a double-pulse electrochemical technique. The resulting electrode was characterized by scanning electron microscopy, energy dispersive X-ray spectroscopy, X-ray diffraction, cyclic voltammetry, and electrochemical impedance spectroscopy. It gives three sharp and well separated oxidation peaks for ascorbic acid (AA), dopamine (DA), and uric acid (UA), with peak separations of 180 and 200 mV for AA-DA and DA-UA, respectively. The sensor enables simultaneous determination of AA, DA and UA with linear responses from 0.6 to 112, 0.1 to 151, and 0.5 to 225 μM, respectively, and with 200, 30 and 150 nM detection limits (at an S/N of 3). The method was successfully applied to the determination of AA, DA, and UA in spiked samples of human serum and urine.

Keywords Multiwalled carbon nanotube · Ionic liquid · Palladium nanoparticle · Simultaneous determination

Electronic supplementary material The online version of this article (doi:10.1007/s00604-014-1293-7) contains supplementary material, which is available to authorized users.

A. A. Rafati (✉) · A. Afraz · A. Hajian · P. Assari
Department of Physical Chemistry, Faculty of Chemistry, Bu-Ali Sina University, P.O. Box 65174, Hamedan, Iran
e-mail: aa_rafati@basu.ac.ir

A. A. Rafati
e-mail: rafati_aa@yahoo.com

Introduction

Ascorbic acid (AA), dopamine (DA) and uric acid (UA) are usually coexisting in biological fluids such as serum and urine. AA is an important antioxidant and deficiency of it may results many disorders. It plays an important role in many biological processes such as free radical scavenging, cancer prevention and immunity improvement [1]. The abnormal concentration levels of DA and UA may also lead to the symptoms of many diseases such as cancer, Parkinson's disease, schizophrenia, gout, pneumonia and cardiovascular disease [2, 3]. Therefore, it is important to detect them selectively and conveniently in routine analysis for developing nerve physiology, making diagnosis and controlling medicine. These three molecules are oxidized at very similar potentials at the traditional electrode, which results in rather poor selectivity. Moreover, they usually foul surface of traditional electrodes and lead to the difficulty of simultaneous measuring them [4]. In order to overcome these problems, several chemically modified electrodes have been used for the sensitive and selective determination of these biomolecules [5–7]. However, due to the importance of AA, UA and DA in biological systems it is still highly desired to prepare novel and more efficient sensors for simultaneous determination of these biomolecules.

In recent years, modification of usual electrodes such as CPE with metallic nanoparticles, carbon nanotubes (CNT) and ILs have shown good effects to improve performance of these electrodes [8–10]. The CNTs have high electrocatalytic effect, fast electron transfer rate, high chemical stability, high surface area and excellent biocompatibility and are extremely attractive in the modification of chemical sensors and biosensors [11–13]. The ILs also as a new green media with high ionic conductivity has been used recently as a new kind of binder

for preparation of CPEs [14]. The IL-modified CPEs have many unique electrochemical properties such as, high conductivity and electron transfer rate, wide electrochemical window and low overpotential [15]. The combination of CNTs and ILs in one electrode also significantly improves the electrocatalytic properties of the modified electrodes [16, 17].

However, using of ILs and CNTs for modification of CPEs must be done carefully. Although, ILs for their conductive nature cause better performance for modified electrodes, but have some unwanted effects in sensors and biosensors. It is observed that the ILs significantly increase background current of modified CPEs [15, 18, 19]. The increase of background current although is desirable in some applications such as super capacitors [20], but may limit application of these electrodes in sensors. The high background current of electrode causes that in the low concentrations the characteristic peaks of many substances overlap by background current and increases detection limit of sensors. The same manner discussed for ILs was observed for using of CNTs in electrodes modification. Although CNTs increase electrochemical properties (especially effective surface area) of modified electrodes, but because their semiconducting nature also increase background current of electrodes [21] that is not desirable in sensing applications. So, according to these opposite effects of CNTs and ILs in modified CPEs, composition of CPE must be effectively optimized regarding to the intended application.

Noble metal nanoparticles, especially palladium nanoparticles (Pd-NPs) effectively can enhance the performance of sensors due to their unusual physical and chemical properties such as good biocompatibility, large effective surface area and unique electronic and catalytic properties [22, 23]. Using of Pd-NPs in modified electrodes can resolve the overlapped voltammetric waves of compounds such as AA and DA into two well-defined voltammetric peaks [24]. Double pulse technique is a simple, fast, and effective method for depositing desired metallic NPs on the electrode surfaces. This method is a recently developed potentiostatic technique that is able to better control over size, morphology, density, and distribution of the metallic NPs by adjusting duration and magnitude of pulse potentials [11]. In this method, nucleation occurs within the first extremely short nucleation pulse with high cathodic polarization and particle growth occurs in the second much longer growth pulse at low cathodic overvoltage [25].

The modified electrodes with CNT and IL or combination of both have shown improved sensitivity and selectivity for determination of AA, DA and UA compared with traditional electrodes [26, 27]. Also, the Pd-NPs have shown significant efficacy for oxidation and determination of these biomolecules [24]. In this work for the first time, the advantages of MWCNTs, IL, and Pd-NPs towards simultaneous determination of AA, UA and DA were utilized in one electrode and systematically were studied. The optimized Pd-NP/MWCNT-IL modified CPE shows high selectivity and sensitivity for simultaneously determination of AA, UA and DA. Also, well separated voltammetric peaks, acceptable accuracies and low detection limits for all species were obtained due to the high electrocatalytic properties of the MWCNTs, IL, and Pd-NPs.

Experimental

Materials

AA, DA, UA, palladium (II) nitrate (Pd $(NO_3)_2$) and 1-Butyl-3-methylpyridinium bis (trifluormethylsulfonyl)imide (≥97 %) were purchased from Sigma (www.sigmaaldrich.com). MWCNTs were purchased from Neutrino (www.neunano.com, Iran, length~50 μm, diameter~8–15 nm, purity>95 %, ash<1.5 %). In order to remove the amorphous carbon and other probable impurities and/or to improve the electron transfer properties and/or to allow further functionalization, MWCNTs were treated before use by a procedure reported previously [10, 12]. Typically, a 500 mg of the MWCNTs were dried in 400 °C for 2 h in nitrogen atmosphere. Then MWCNTs were dispersed in 50 mL of 6.0 M HCl for 2 h under ultrasonic agitation under the nitrogen atmosphere. The dispersed MWCNTs filtered on a Wattman 42 filter paper and washed with deionized water until the pH of the solution was neutral, and finally were dried under the IR lamp. Graphite powder with a 10 μm particle size and highly pure paraffin (both were purchased from Merck) was used for preparation of carbon paste electrodes. All other reagents were of analytical grade from Merck. The stock solutions of AA (0.03 M), DA (0.01 M) and UA (0.01 M) were prepared daily in deionized water. UA was dissolved in a small volume of 0.1 M NaOH solution and diluted to 0.01 M concentration. Phosphate buffer solutions (PB, 0.1 M) were prepared from H_3PO_4, KH_2PO_4 and K_2HPO_4 and pH values were adjusted with HCl and KOH solutions.

Apparatus and procedures

Electrochemical experiments were performed with a computer-controlled μ-Autolab modular electrochemical system (PGSTAT101, the Netherlands), driven with NOVA Software (upgrade 1.10). A conventional three-electrode cell was used with an Ag/AgCl, sat. KCl as reference electrode, a platinum plate as counter electrode (all from Azar electrode Co., Iran), and prepared CPEs as working electrode. Scanning electron microscopy (SEM) and energy dispersive X-ray spectroscopy (EIS) analysis were obtained using a VEGA TESCAN SEM. X-ray diffraction (XRD) pattern of sample was collected by an X-ray diffractometer ITAL STRUCTURES model APD2000 with applying Cu Kα radiation wavelength.

Preparation of the CPEs

The modified CPEs were prepared by hand mixing of graphite powder, pretreated MWCNT, paraffin oil and IL with various ratios (w/w) in a mortar for at least 15 min. The pastes were packed into the end of a polyamide tube (2 mm diameter). Electrical contact was made by forcing a copper pin down into the polyamide tube and into the back of the composite. A new surface was obtained by smoothing the electrode onto a weighing paper and rinsed carefully with deionized water prior to each measurement.

Electrodeposition of palladium nanoparticles

The potentiostatic double-pulse technique was used for electrodeposition of Pd-NPs onto the CPE surface from a deareated KNO_3 solution (0.1 M) containing 0.25 mM Pd $(NO_3)_2$. The pulse parameters for chronoamperometry adjusted as follow:

$$\text{Nucleation pulse}: E_1 = -0.2\,\text{V vs Ag/AgCl}; t_1 = 25\,\text{ms}$$

$$\text{Growth pulse}: E_2 = 0.2\,\text{vs Ag/AgCl}; t_2 = 120\,\text{s}$$

The prepared electrode was thoroughly washed with deionized water and dried before use.

Results and discussion

Optimize formulation of carbon paste electrode

The composition of modified CPE was optimized by preparation and electrochemically investigation of various modified CPEs presented in Table 1. For electrochemically investigations the CVs of these electrodes are provided in 0.1 M KNO_3 solution containing 1.0 mM $K_3[Fe(CN)_6]$ at various scan rates. The obtained electrochemical parameters of each CPE are ΔE (mV), capacitance, cathodic peak height (I_{pc}, μA) and effective surface area. The ΔE and I_{pc} were obtained directly from CVs with scan rate of 50 mV s^{-1}. The effective surface area was calculated from Randles-Sevcik equation (at 25 °C) [25]:

$$i_p = \left(2.69 \times 10^5\right) n^{3/2} A C_m D^{1/2} v^{1/2} \quad (1)$$

where n is the number of electrons, A is the effective surface area (in cm^2), C_m is the bulk concentration (in mol cm^{-3}), D is the diffusion coefficient (that for $[Fe(CN)_6]^{-3}$ is 8.96×10^{-6} cm^2 s^{-1} [29]), and v is the scan rate (in V s^{-1}). From slope of peak current (i_p, in A) versus square root of scan rates and according Eq. 1, the surface area was calculated for various CPEs. The capacitance of each CPE was calculated on the basis of following Eq. 2[27]:

$$C = \int I(E)dE \,/(2v(E_2 - E_1)) \quad (2)$$

where C is capacitance (in farad (F)), $I(E)$ is the instantaneous current (in A), $\int I(E)dE$ is the total voltammetric charge obtained by integration of positive and negative sweep in CVs (0.1 M KNO_3, 1.0 mM $K_3[Fe(CN)_6]$, 50 mV s^{-1}) except faradic peaks portions, E_1, E_2 are the cutoff potentials in CVs, and 2 (E_2-E_1) is the total potential width in positive and negative sweeps (in V).

The calculated ΔE, I_{pc}, capacitance and surface area are shown in Table 1 and can be analyzed for obtain optimized composition of modified CPE. The goals of responses are minimum for ΔE and capacitance, and maximum for I_{pc} and surface area. In number 1–4 electrodes effect of MWCNT percentage on the electrode performance can be investigated. In these electrodes, by increasing MWCNT percentage, the ΔE was decreased, and the I_{pc} and surface area were increased that all are desired for a sensor. The lower ΔE reflects higher electron transfer rate, and the higher I_{pc} and surface area reflect higher effective surface area for electrode. Because low density and high surface area of MWCNTs, by increasing percentage of MWCNTs the percentage of paraffin must be increased for obtain a polishable and stable surface for modified electrode. This decreases the modified electrode electrochemical performance. On the other hand, the semiconducting nature of MWCNTs has caused the slowly increasing background current of modified CPE by increasing MWCNT percentage. However, modified CPE with 10 % MWCNT shows best properties for application in sensors.

Effect of percentage of ionic liquid on the modified electrode performance can be also investigated with comparison data of number 3, and number 5–8 electrodes (Table 1). With increasing percentage of IL the ΔE was decreased, and the I_{pc} and surface area were increased that all are desired for a sensor. In the other hand increasing of IL significantly increase capacitance (or background current) of modified electrode that is not acceptable in analytical applications. The effect of IL in capacitance of electrode is so important. Fig. 1a shows the CV of number 8 modified electrode with composition of 75 % graphite and 25 % IL (Table 1). The CV shape of this modified electrode is nearly rectangular that indicates the ideal double layer capacitor behavior for it [20]. Overall the modification of CPE with 10 % IL in two aspects is appropriate: (1) improved electrochemical properties for electrode such as lower ΔE and higher I_{pc} rather than traditional CPE, (2) the lowest possible background current that is acceptable in sensing applications. Consequently the final optimized composition for CPE was obtained as follow: 60 % graphite, 20 % paraffin, 10 % MWCNT and 10 % IL. Fig. 1b shows the CVs of optimized CPE and conventional

Table 1 Calculated electrochemical parameters (E, I_{pc}, capacitance and surface area) of modified electrodes with different compositions

Num.	Graphite%	MWCNT%	Paraffin%	IL%	E (mV)	Area (cm^2)	Capacitance (F)	I_{pc} (A)
1	75	0	25	0	237.1	0.01	1.6	3.54
2	70	5	25	0	205.1	0.03	20.0	5.10
3	60	10	30	0	173.0	0.07	21.4	7.01
4	50	15	35	0	185.9	0.08	47.6	7.93
5	60	10	25	5	147.4	0.09	156.6	9.31
6	60	10	20	10	121.8	0.11	176.3	15.53
7	60	10	15	15	109.0	0.15	537.9	19.00
8	75	0	0	25	90.0	0.08	1,812.3	21.26

CPE (75 % graphite, 25 % paraffin) in 0.1 M KNO_3 containing 1.0 mM $K_3[Fe(CN)_6]$. The optimized CPE show low ΔE and consequently high electron transfer rate, acceptable capacitance, very higher effective surface area, and very distinguish peaks rather than conventional CPE.

Electrodeposition of palladium nanoparticles

Electrodeposition of palladium nanoparticles carried out by using a double pulse technique. In this method, nucleation occurs within the first extremely short nucleation pulse with high cathodic polarization and particle growth occurs in the second much longer growth pulse at low cathodic overvoltage [11]. In this method the pulse potentials must be obtained from CVs of palladium precursor solution. The potential of nucleation pulse adjusts at more negative values than Pd deposition potential in first scan, and the growth pulse must adjust more positively than nucleation pulse but more negatively than potential that Pd begins dissolution. In this case, the growth of Pd just occurs on the Pd nuclei formed during the first pulse. Fig. 2 shows the first and second CV scans of 0.25 mM $Pd(NO_3)_2$ in 0.1 M KNO_3 solution on optimized CPE (60 % graphite, 20 % paraffin, 10 % MWCNT and 10 % IL). For the first scan, the cathodic peak at −0.04 V (vs. Ag/AgCl) is resulted from the reduction of Pd^{2+}. At the subsequent scan, reduction of Pd^{2+} occurs at smaller overpotential (0.22 V) because the Pd^{2+} reduces on the deposited palladium nucleus at the first scan. The peak at −0.27 V shows the reduction process of protons to hydrogen, and the peak at −0.21 V shows the oxidation of hydrogen atoms which are adsorbed on the Pd surface, respectively in negative and positive directions on scanning potential [31]. These peaks confirm the Pd nucleation process on the electrode surface. Because adsorption hydrogen atoms on the deposited Pd

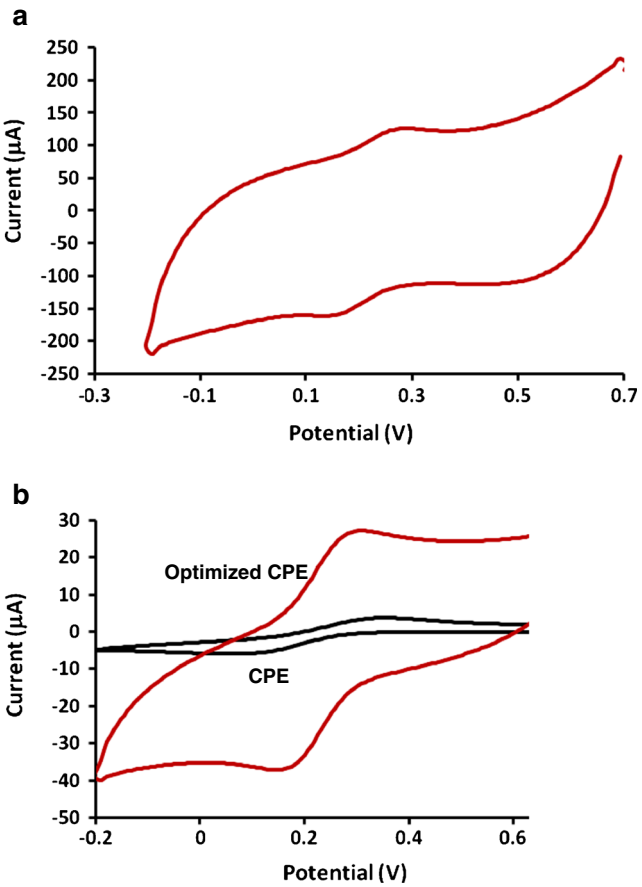

Fig. 1 **a** CV of number 8 prepared modified electrode with composition of 75 % graphite and 25 % IL, **b** CVs of OCPE and CPE in 0.1 M KNO_3 containing 1.0 mM $K_3[Fe(CN)_6]$, scan rate of 50 $mV \cdot s^{-1}$

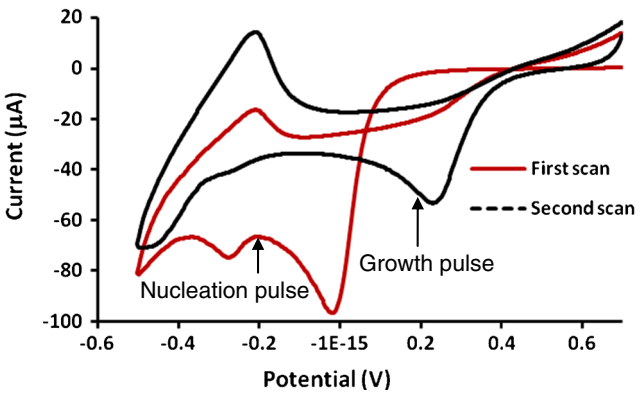

Fig. 2 First and second CV scans of 0.25 mM $Pd(NO_3)_2$ in 0.1 M KNO_3 solution on OCPE, with scan rate of 50 $mV \cdot s^{-1}$

nucleus at the potentials lower than −0.27 V, nucleation pulse must be more positive than this potential for effectively deposit Pd nucleus. According to these potentials and discussed fundamentals of the double-pulse technique, the values of pulse potentials from Fig. 2 were selected as −0.2 V for nucleation and 0.2 V for growth pulse with 0.025 and 120 s duration, respectively. These values set as chronoamperometry parameters for Pd-NPs electrodeposition onto surface of optimized CPE from 0.25 mM $Pd(NO_3)_2$ in 0.1 M KNO_3 solution.

Characterization of modified optimal CPE by palladium nanoparticles

Figure 3a, b and c shows the SEM images of Pd-NPs deposited on optimized CPE (Pd-NP/CPE). From these figures the deposited Pd-NPs have lower than 50 nm diameter with a very dense distribution. This specific surface causes high surface area and improved electrocatalytic properties for Pd-NP/CPE. The EDS analysis (Fig. 3d) shows that the surface of prepared Pd-NP/CPE contained C, O, F and Pd elements with 88.60, 8.43, 1.65 and 1.32 wt.%, respectively. Presence of fluorine is related to use of IL in optimized CPE and low percentage of Pd confirms NPs structure of deposited Pd on the modified electrode surface. Also this low percentage of Pd significantly decreases cost of final sensor.

The X-ray diffraction pattern of the Pd-NP/CPE is shown in Fig. 3e. The peaks at 40.0° (111), 47.7° (200), 68.4° (220), 83.3° (311) and 86.9° (222) are in agreement with the corresponding standard cards for face-centered cubic structure of Pd crystals (JCPDS, file no. 05–0681) [32]. The peaks at 26.5° (002), 43.3° (100), 44.8° (101) and 54.6° (004) represent the carbon backbone of the CPE (JCPDS, file no. 08–

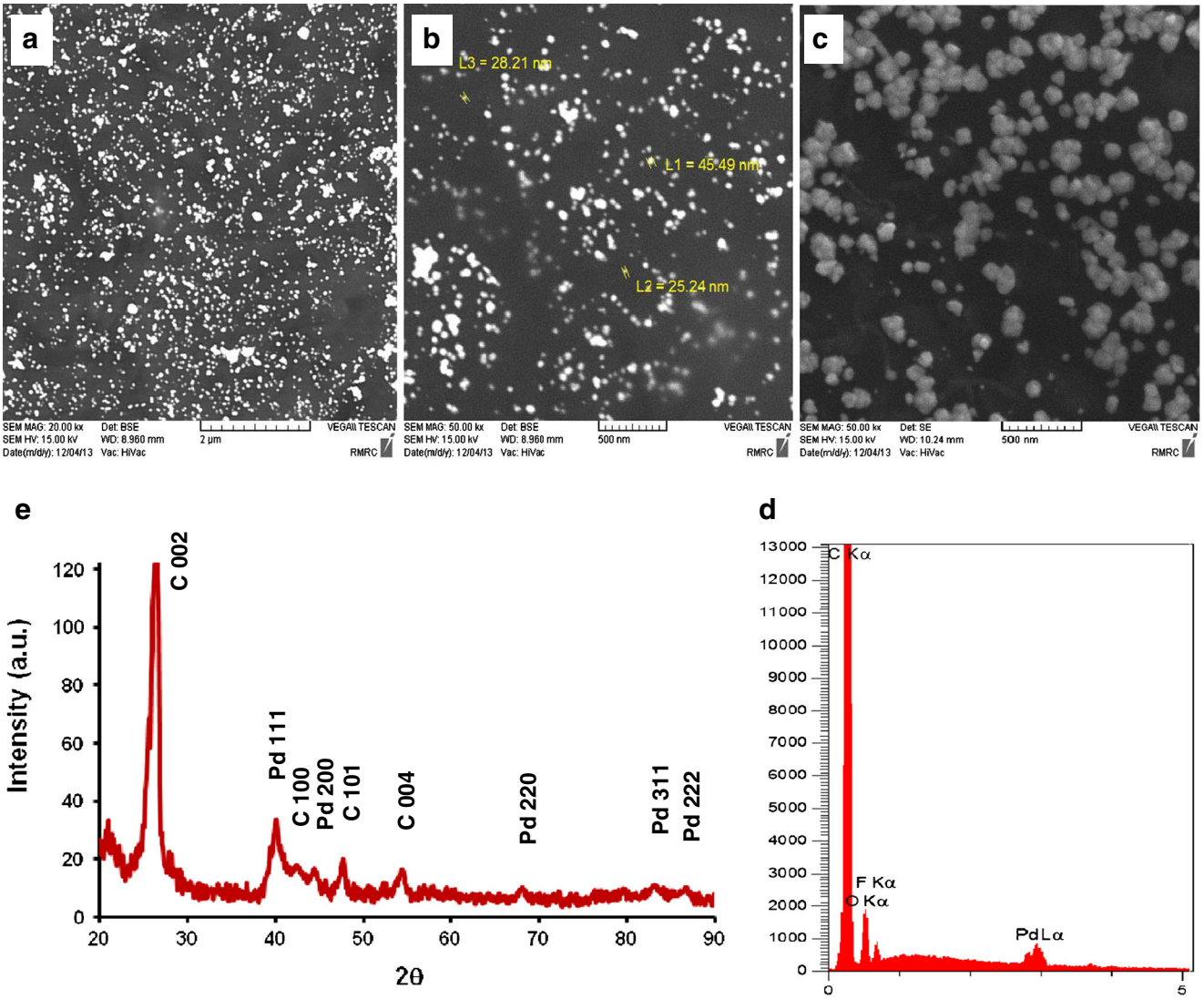

Fig. 3 **a**, **b** and **c** SEM images of PNPs deposited on OCPE with various magnification, **d** EDS spectrum and **e** X-ray diffraction pattern of the PNP/OCPE

0415) [33]. The average crystalline sizes obtained from X-powder software according the Debye-Scherrer's equation is 4 nm for Pd-NPs.

The electron transfer kinetics of a redox probe at the modified electrodes was studied with EIS measurements. EIS include a semicircle part and a linear part: the semicircle part at high frequencies is corresponding to the electron transfer limited process and the linear part at low frequencies is corresponding to the diffusion process [34]. Fig. S1 (see supplementary data) shows the impedance spectra in the form of Nyquist diagrams for three different electrodes in 0.1 M KCl solution containing 5.0 mM $K_3[Fe(CN)_6]$ at open circuit. To clearly understand of the electrical properties of the electrodes/solution interfaces the Randle's equivalent circuit (inset of Fig. S1, bottom) was chosen to fit the obtained impedance data. In this model the semicircle diameter equals with charge transfer resistance (R_{ct}) and exhibits the electron transfer kinetics of the redox probe at electrode interface. As shown in Fig. S1, the very lower R_{ct} of optimized CPE (127 Ω) rather than traditional CPE (2,571 Ω) is due to using of IL with high conductivity in construction of this electrode. This observation is consistent with that observed in Fig. 1b and reconfirms that this composition could facilitate the charge transfer. Also the lower R_{ct} of Pd-NP/CPE (107 Ω) rather than optimized CPE shows that the Pd-NPs can be used to construct high efficient electrochemical sensors as significant electrochemical active materials that make electron transfer easier.

Electrocatalytic response to AA, DA and UA

It shall be noted here that the AA, DA and UA are present in ionic forms in solution depending on its pH value. At the pH applied here, AA is present as the anion (ascorbate), DA as a cation (due to protonation of the amino group), while UA is uncharged but becomes anionic at pH 7. Fig. 4a presents the differential pulse voltammograms (DPVs) of three different electrodes in PB with 20 μM AA, 25 μM DA and 22 μM UA. At the conventional CPE determination of UA in presence of AA and DA is possible, but oxidation peaks of AA and DA were strongly overlapped. For the optimized CPE despite that the intensity of peaks is increased, the simultaneous determination of these compounds is still impossible. However, the Pd-NP/CPE shows three distinct peaks for AA, DA and UA that can well be used for simultaneous determination of these molecules. For further investigation the CVs of Pd-NP/CPE and conventional CPE were studied in PB with 120 μM AA, 120 μM DA and 100 μM UA (Fig. 4b and c). At the CPE single AA and DA are oxidized in 0.35 and 0.54 V, respectively (Fig. 4c). In simultaneous study, the oxidation peaks of AA and DA overlapped and CPE cannot separate the peaks of them. Compared with the CPE, at the Pd-NP/CPE because high electrocatalytic properties and large electroactive surface area of Pd-NPs peaks of AA and DA were shifted to more negative values (0.18 and 0.38 V, respectively) and effectively were separated. Figure 4d shows roles of any modification steps in the performance of modified electrode for simultaneous determination. In the first step, modification of CPE with MWCNT and IL enhances effective surface area of modified electrode and increases intensity of peaks. In the next step modification of optimized modified CPE with Pd-NPs facile oxidation of AA, DA and UA, and caused that three well separated oxidation peaks for these molecules were appeared.

Effect of pH

The influence of pH on simultaneous determination of AA (20 μM), DA (25 μM) and UA (22 μM) with Pd-NP/CPE was studied in PB by DPV (Fig. 4e). It was observed that as pH of solutions were increased, the peak potentials shift toward more negative values, suggesting the involvement of proton in the AA, DA and UA oxidation reactions. The peak separations for $\Delta E_{AA\text{-}DA}$, $\Delta E_{DA\text{-}UA}$, and $\Delta E_{AA\text{-}UA}$, are 200, 180 and 380 mV in pH 3.0, 180, 200 and 380 mV in pH 4.5, and 160, 180 and 340 mV in pH 5.5, respectively. According to these peak separation values, peak currents, and for better compatibility with biological systems, pH 4.5 was chosen for construction of calibration curve and for simultaneous determination of AA, DA and UA in standard solution and biological samples.

Effect of scan rate

The kinetics of electrode reactions were investigated by using CVs of the Pd-NP/CPE at different scan rates for 120 μM AA, 120 μM DA and 100 μM UA in PB (0.1 M, pH=4.5, Fig. S2). Insets of Fig. S2 show that the peak currents changed in a linear relationship with the square root of scan rates in ranges of 10–400, 10–1,500, and 10–600 mV s^{-1} for AA, DA and UA, respectively, and by R-squared values of above 0.99 for all analytes. These plots indicate that the electrochemical reactions for these molecules are diffusion controlled and the electron transfer rate for Pd-NP/CPE is fast. Also for more investigations, log peak currents versus log scan rates were plotted for AA, DA, and UA. For these plots when the slope is 0.5, the electrochemical reaction is a diffusion controlled process, and when equals to 1, the electrochemical reaction occurs via an adsorption-controlled process [35]. From insets of Fig. S2 the plots of log anodic peak currents versus log scan rates have slopes of 0.393, 0.520 and 0.392 for AA, DA and UA, respectively. These values show that the electrochemical reactions for these biomolecules are governed by diffusion control and the surface of Pd-NP/CPE was not fouled by them.

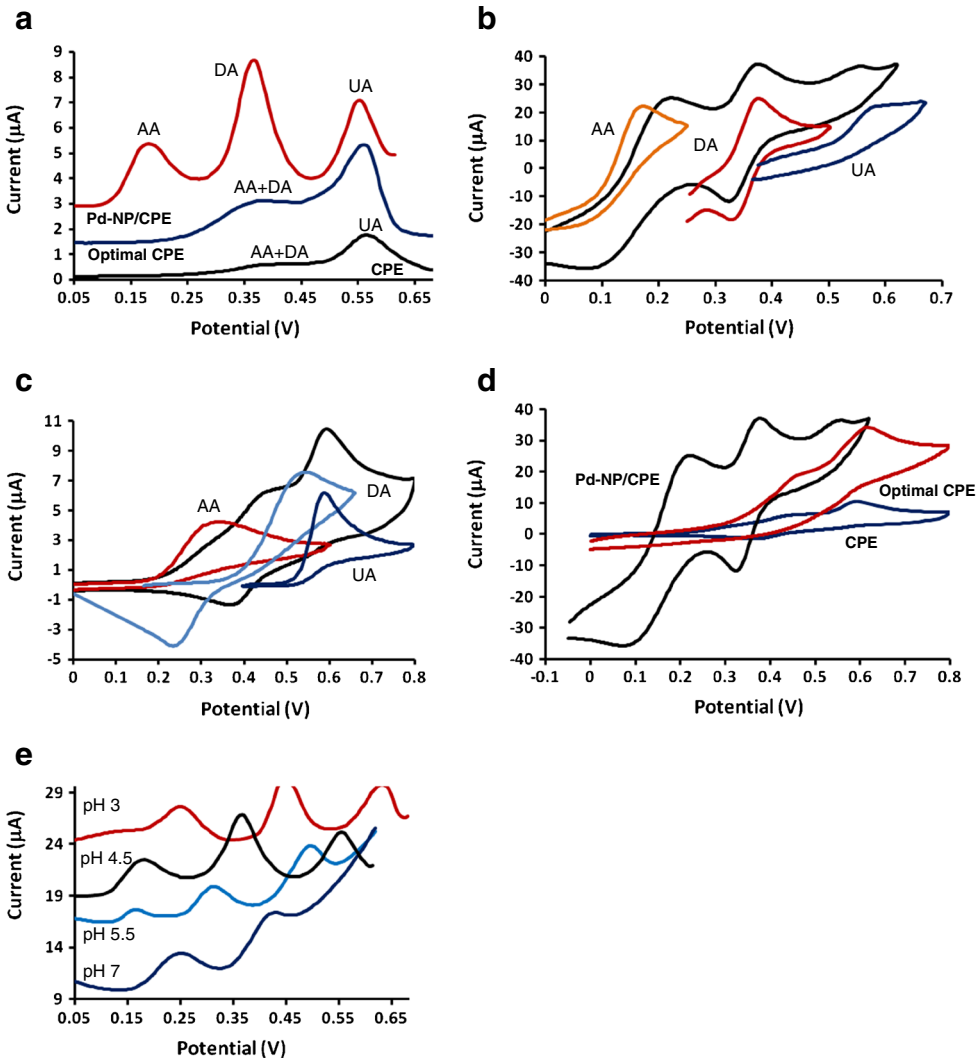

Fig. 4 **a** DPVs of CPE, OCPE and PNP/OCPE in PBS (pH=4.5) with 20 μM AA, 25 μM DA and 22 μM UA. CVs of **b** PNP/OCPE, **c** CPE, **d** PNP/OCPE, OCPE and CPE in PBS (pH=4.5) with 120 μM AA, 120 μM DA and 100 μM UA. **e** DPV of PNP/OCPE in various pH for 20 μM AA, 25 μM DA and 22 μM UA. All with scan rate of 50 $mV \cdot s^{-1}$

Determination of AA, DA and UA

Simultaneous determination of UA, AA and DA at Pd-NP/CPE was carried out by using DPV method. In the first experiment (Fig. 5a, b and c), only concentration of one species was changed, while concentrations of the other two species were kept constant in PB (0.1 M, pH=4.5). The linear range for the determination of AA is 0.6-112 μM with the sensitivity of 0.114 μA μM^{-1}, R-squared value of 0.997, and the detection limit of 0.2 μM (at an S/N of 3)). For determination of DA the linear range is 0.1-151 μM with the sensitivity of 0.148 μA μM^{-1}, R-squared value of 0.998, and the detection limit of 0.03 μM. The determination of UA show a linear ranges from 0.5 to 225 μM with the sensitivity of 0.115 μA μM^{-1}, R-squared value of 0.997, and the detection limits of 0.15 μM. In another experiment when the concentrations of all species were changed in the PB, the electrooxidation of AA, DA and UA were investigated and the results are shown in Fig. 5d. From this figure for AA, DA and UA the sensitivity values obtained as 0.104, 0.152, and 0.114 μA μM^{-1}, respectively, with R-squared values of 0.998, 0.997, and 0.996. In this figure the slope of the linear regression line for the calibration curve of each species is nearly equal to that only concentration of one species was changed, indicating that AA, DA and UA do not interfere in the determination of each other. The percent relative standard deviation (% RSD) for ten determinations of 10 μM AA, 10 μM DA, and 10 μM UA by using ten fresh modified electrodes were 4.0, 3.7, and 4.5 %, respectively. Stability of the Pd-NP/CPE was also investigated after electrode storage in PB at room temperature for two week. The response of modified electrode lost approximately 4.7 %, 4.6 % and 4.2 % of its original response for AA, DA and UA, respectively. Thus, the suggested electrode showed a good repeatability and high stability.

Table S1 shows a comparison between previously reported electrochemical methods and the suggested method in this work for the simultaneous determination of AA, DA and

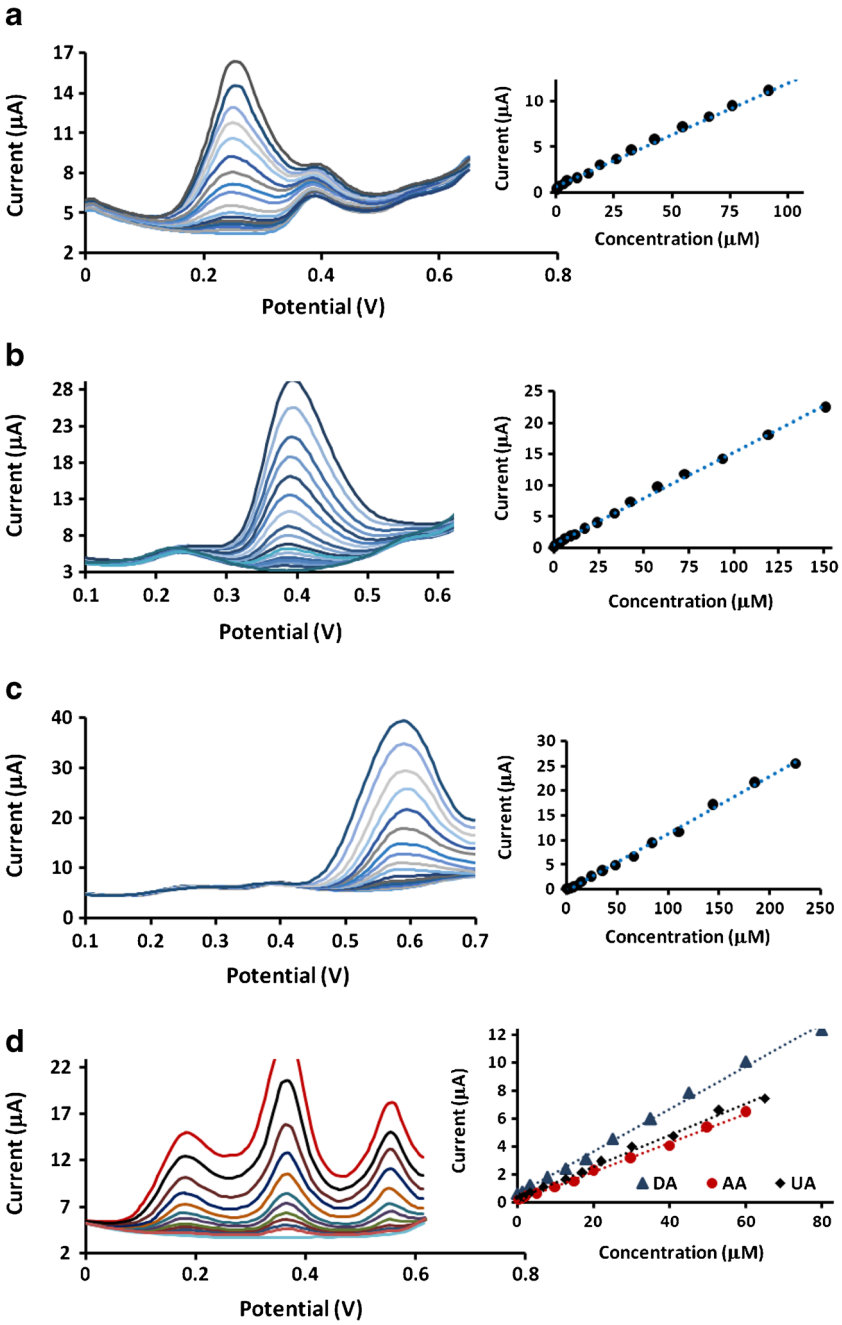

Fig. 5 DPVs and calibration curves of PNP/OCPE in PBS (0.1 M, pH=4.5) containing **a** 6 μM DA, 3 μM UA and various concentration of AA from 0.6 to 112 μM, **b** 6 μM AA, 3 μM UA and various concentration of DA from 0.1 to 150 μM, **c** 6 μM AA and 6 μM DA and various concentration of UA from 0.5 to 225 μM, **d** various concentration of AA, DA and UA from 0.5 to 60 μM, 0.08 to 80 μM and 0.5 to 65 μM, respectively. All with scan rate of 50 $mV \cdot s^{-1}$

UA. The wide linear response range and the low detection limit cause that the prepared sensor in this work be comparable with previous works. The suggested modified electrode in this work shows a symmetric state for the peak separations rather than some previously reported modified electrodes that caused improving linear ranges for this sensor. The efficient catalytic property of Pd-NP/CPE to AA, DA and UA could be attributed to the high electrocatalytic property and large electroactive surface area of Pd-NPs, and the synergistic amplification effect of the two kinds of nanomaterials and ionic liquid.

Real samples analysis

The Pd-NP/CPE was applied to analysis human serum and urine as real samples by using the standard addition method. The urine and plasma samples were respectively diluted 50 and 30 times with PB (0.1 M, pH=4.5) before the measurement to fit the calibration curve and also reduce the matrix effect. The determination of each species was performed by using DPV and results are presented in Table 2. According to these results, the suggested method could be effectively used for the determination of AA, DA and UA in real samples.

Table 2 Results of the recovery analysis of AA, DA and UA in real samples by using Pd-NP/CPE as working electrode

Sample		Detected[a] (M)	Spiked (M)	Found[a] (M)	Recovery (%)
Urine1[b]	AA	–	20	19.8±0.4	99.0
	DA	–	20	19.2±0.2	96.0
	UA	58.2±1.0	15	73.7±1.2	104.0
Urine2[b]	AA	–	30	29.7±0.8	99.0
	DA	–	30	29.4±0.4	98.0
	UA	52.3±0.8	20	72.9±0.9	103.0
Serum[c]	AA	–	15	14.7±0.7	98.0
	DA	–	15	14.6±0.1	97.3
	UA	10.2±0.3	15	24.6±0.3	96.0

[a] mean±standard deviation (n=3)

[b] diluted 50 times with PB (0.1 M, pH=4.5)

[c] diluted 30 times with PB (0.1 M, pH=4.5)

Conclusions

In summary, a modified CPE with MWCNT and IL was prepared. The optimized composition of modified CPE was determined by electrochemical studies. The optimized CPE, with formulation of 60 % graphite, 20 % paraffin, 10 % MWCNT, and 10 % IL shows good electrochemical properties that are well matched with model prediction parameters. In a next step, the optimized CPE was further modified with Pd-NP by applying a double pulse electrochemical technique. The resulting electrode was characterized by SEM, EDS, XRD, and EIS techniques. The specific nanostructure of deposited palladium with a dense distribution caused high surface area and electrocatalytic activity for modified electrode. The EDS analysis indicated that the electrodeposited Pd-NPs have only 1.32 wt.% of surface that will decrease cost of final sensor. The electrochemical studies revealed that the electrocatalytic properties and large electroactive surface area of the Pd-NP facile oxidation of AA and DA, and caused peaks of them shifted to more negative values and were effectively separated. The scan rate investigations of AA, DA and UA showed that these molecules do not foul surface of prepared sensor, the oxidation reactions of them are diffusion controlled, and the electron transfer rate for modified electrode is fast. The modified electrode gives three sharp and discriminate oxidation peaks for AA, DA and UA with peak separations of 180, 200 and 380 mV in pH 4.5 for $\Delta E_{AA\text{-}DA}$, $\Delta E_{DA\text{-}UA}$ and $\Delta E_{AA\text{-}UA}$, respectively. The sensor enables simultaneous determination of AA, DA and UA with linear responses from 0.6 to 112, 0.1 to 151, and 0.5 to 225 μM, respectively, and with 200, 30 and 150 nM detection limits (at an S/N of 3). The prepared sensor also shows good stability and repeatability, and effectively was applied to the determination of AA, DA, and UA in spiked samples of human serum and urine.

Acknowledgments The authors greatly acknowledge Bu-Ali Sina University for the financial support from the Grant Research Council.

References

1. Ping J, Wu J, Wang Y, Ying Y (2012) Simultaneous determination of ascorbic acid, dopamine and uric acid using high-performance screen-printed graphene electrode. Biosens Bioelectron 34:70–76
2. Zheng Y, Huang Z, Zhao C, Weng S, Zheng W, Lin X (2013) A gold electrode with a flower-like gold nanostructure for simultaneous determination of dopamine and ascorbic acid. Microchim Acta 180: 537–544
3. Rouhollahi A, Rajabzadeh R, Ghasemi J (2007) Simultaneous determination of dopamine and ascorbic acid by linear sweep voltammetry along with chemometrics using a glassy carbon electrode. Microchim Acta 157:139–147
4. Sheng Z-H, Zheng X-Q, Xu J-Y, Bao W-J, Wang F-B, Xia X-H (2012) Electrochemical sensor based on nitrogen doped graphene: simultaneous determination of ascorbic acid, dopamine and uric acid. Biosens Bioelectron 34:125–131
5. Sun C-L, Chang C-T, Lee H-H, Zhou J, Wang J, Sham T-K, Pong W-F (2011) Microwave-assisted synthesis of a core–shell MWCNT/GONR aheterostructure for the electrochemical detection of ascorbic acid, dopamine, and uric acid. ACS Nano 5:7788–7795
6. Wang G, Sun J, Zhang W, Jiao S, Fang B (2009) Simultaneous determination of dopamine, uric acid and ascorbic acid with LaFeO3 nanoparticles modified electrode. Microchim Acta 164: 357–362
7. Wang Y, Xiao Y (2012) Glassy carbon electrode modified with poly (dibromofluorescein) for the selective determination of dopamine and uric acid in the presence of ascorbic acid. Microchim Acta 178: 123–130
8. Janegitz BC, Marcolino-Junior LH, Campana-Filho SP, Faria RC, Fatibello-Filho O (2009) Anodic stripping voltammetric determination of copper (II) using a functionalized carbon nanotubes paste electrode modified with crosslinked chitosan. Sens Actuators B 142: 260–266
9. Afkhami A, Madrakian T, Shirzadmehr A, Tabatabaee M, Bagheri H (2012) New schiff base-carbon nanotube-nanosilica-ionic liquid as a high performance sensing material of a potentiometric sensor for nanomolar determination of cerium (III) ions. Sens Actuators B 174:237–244
10. Bagheri H, Afkhami A, Khoshsafar H, Rezaei M, Shirzadmehr A (2013) Simultaneous electrochemical determination of heavy metals using a triphenylphosphine/MWCNTs composite carbon ionic liquid electrode. Sens Actuators B 186:451–460
11. Afraz A, Rafati A, Hajian A (2013) Analytical sensing of hydrogen peroxide on Ag nanoparticles-multiwalled carbon nanotube-modified glassy carbon electrode. J Solid State Electrochem 17: 2017–2025
12. Valentini F, Amine A, Orlanducci S, Terranova ML, Palleschi G (2003) Carbon nanotube purification: preparation and characterization of carbon nanotube paste electrodes. Anal Chem 75:5413–5421
13. Rafati AA, Afraz A (2014) Amperometric sensing of anti-HIV drug zidovudine on Ag nanofilm-multiwalled carbon nanotubes modified glassy carbon electrode. Mater Sci Eng C 39:105–112
14. Maleki N, Safavi A, Tajabadi F (2006) High-performance carbon composite electrode based on an ionic liquid as a binder. Anal Chem 78:3820–3826
15. Sun W, Yang M, Jiao K (2007) Electrocatalytic oxidation of dopamine at an ionic liquid modified carbon paste electrode and its analytical application. Anal Bioanal Chem 389:1283–1291

16. Xi M, Duan Y, Li X, Qu L, Sun W, Jiao K (2010) Carbon electrode modified with ionic liquid and multi-walled carbon nanotubes for voltammetric sensing of adenine. Microchim Acta 170:53–58
17. Zhan X-M, Liu L-H, Gao Z-N (2011) Electrocatalytic oxidation of quinine sulfate at a multiwall carbon nanotubes-ionic liquid modified glassy carbon electrode and its electrochemical determination. J Solid State Electrochem 15:1185–1192
18. Xiao F, Ruan C, Li J, Liu L, Zhao F, Zeng B (2008) Voltammetric determination of xanthine with a single-walled carbon nanotube-ionic liquid paste modified glassy carbon electrode. Electroanalysis 20:361–366
19. Sun W, Gao R, Jiao K (2007) Electrochemistry and electrocatalysis of hemoglobin in nafion/nano-CaCO3 film on a new ionic liquid $BPPF_6$ modified carbon paste electrode. J Phys Chem B 111:4560–4567
20. Liu C, Yu Z, Neff D, Zhamu A, Jang BZ (2010) Graphene-based supercapacitor with an ultrahigh energy density. Nano Lett 10: 4863–4868
21. Li J, Cassell A, Delzeit L, Han J, Meyyappan M (2002) Novel three-dimensional electrodes: electrochemical properties of carbon nanotube ensembles. J Phys Chem B 106:9299–9305
22. Palanisamy S, Ku S, Chen S-M (2013) Dopamine sensor based on a glassy carbon electrode modified with a reduced graphene oxide and palladium nanoparticles composite. Microchim Acta 180:1037–1042
23. Łuczak T, Bełtowska-Brzezinska M (2011) Gold electrodes modified with gold nanoparticles and thio compounds for electrochemical sensing of dopamine alone and in presence of potential interferents. A comparative study. Microchim Acta 174:19–30
24. Huang J, Liu Y, Hou H, You T (2008) Simultaneous electrochemical determination of dopamine, uric acid and ascorbic acid using palladium nanoparticle-loaded carbon nanofibers modified electrode. Biosens Bioelectron 24:632–637
25. Ueda M, Dietz H, Anders A, Kneppe H, Meixner A, Plieth W (2002) Double-pulse technique as an electrochemical tool for controlling the preparation of metallic nanoparticles. Electrochim Acta 48:377–386
26. Yan Q, Zhao F, Li G, Zeng B (2006) Voltammetric determination of uric acid with a glassy carbon electrode coated by paste of multiwalled carbon nanotubes and ionic liquid. Electroanalysis 18: 1075–1080
27. Sun Y, Fei J, Hou J, Zhang Q, Liu Y, Hu B (2009) Simultaneous determination of dopamine and serotonin using a carbon nanotubes-ionic liquid gel modified glassy carbon electrode. Microchim Acta 165:373–379
28. Wang J (2004) Analytical electrochemistry. Wiley
29. Lide DR (2004) CRC handbook of chemistry and physics 2004–2005: A ready-reference book of chemical and physical data. CRC PressI Llc
30. Chen W, Fan Z, Gu L, Bao X, Wang C (2010) Enhanced capacitance of manganese oxide via confinement inside carbon nanotubes. Chem Commun 46:3905–3907
31. Thiagarajan S, Yang R-F, Chen S-M (2009) Palladium nanoparticles modified electrode for the selective detection of catecholamine neurotransmitters in presence of ascorbic acid. Bioelectrochemistry 75: 163–169
32. Jiang L, Hsu A, Chu D, Chen R (2009) Size-dependent activity of palladium nanoparticles for oxygen electroreduction in alkaline solutions. J Electrochem Soc 156:B643–B649
33. Liang C, Xia W, Soltani-Ahmadi H, Schluter O, Fischer RA, Muhler M (2005) The two-step chemical vapor deposition of Pd (allyl) Cp as an atom-efficient route to synthesize highly dispersed palladium nanoparticles on carbon nanofibers. Chem Commun :282–284
34. Zhang L, Zhang C, Lian J (2008) Electrochemical synthesis of polyaniline nano-networks on p-aminobenzene sulfonic acid functionalized glassy carbon electrode: its use for the simultaneous determination of ascorbic acid and uric acid. Biosens Bioelectron 24:690–695
35. Nematollahi D, Zohdijamil Z, Salehzadeh H An efficient electrochemical method for the synthesis of N,N,N',N'-tetraalkyl-4,4'-azodianiline. J Electroanal Chem